On the nozzle geometry of a transferred plasma cutting torch for the arc stabilization with swirl flow

Sakuragi, Shunichi
Komatsu Ltd.

https://doi.org/10.15017/17376

出版情報：九州大学大学院総合理工学報告. 17 (2), pp.229-236, 1995-09-01. Interdisciplinary Graduate School of Engineering Sciences, Kyushu University

九州大学大学院総合理工学研究科報告
第17巻 第2号 229-236頁 平成7年9月

Engineering Sciences Reports, Kyushu University
(KYUSHU DAIGAKU SOGORIKOGAKU KENKYUKA HOKOKU)
Vol. 17, No. 2, pp. 229-236, SEPT 1995

On the nozzle geometry of a transferred plasma cutting torch for the arc stabilization with swirl flow

Shunichi SAKURAGI*

(Received May 31, 1995)

In the plasma cutting process, the arcjet with high specific energy is required to get good cut quality in the dross-free cutting. For this purpose, it is necessary to stabilize the arc with gas flow rate lower than the conventional torches. The present paper discusses the nozzle shape that effectively stabilizes the arc by the swirl flow. The pressure measurement inside the large-scale model-nozzle indicates that the nozzle shape can be optimized to create a large pressure gradient for the arc stabilization with a constant gas flow rate. The metal cutting test by the nozzle with optimum shape shows a remarkable improvement in arc stabilization.

1. Introduction

The arc stabilization by the swirl flow has been used in the various types of plasma torches[1]. The arc stabilization in a torch is very important for the stable operation of the plasma cutter. However, the characteristics of the swirl flow inside a plasma torch has not been well understood, and the geometry of the torch has not been optimized for the effective generation of the swirl flow. If the arc is stabilized by a swirl flow with a small flow rate, it is possible to increase the specific energy of the transferred arcjet. This contributes to the cut quality in plasma cutting process, especially to the dross-free cutting[2].

To realize the dross-free cutting, it is necessary[2] to develop a new torch that stabilizes the arc with the flow rate lower than the critical value where the flow is considered laminar. To stabilize an arc effectively, it is required to optimize the geometry of the discharge space, where the arc is sustained with the high pressure gas wall created by the swirl flow. The centrifugal force of the swirl flow creates large pressure gradient in the discharge space, and this force takes a minimum value at the center of the torch and a maximum value on the surface of the nozzle wall. An arc column is stably sustained in the low pressure region near the center of a torch. The parameter that expresses the effect of a swirl flow is static pressures on the wall surfaces of the nozzle and electrode which constitute the discharge space in the torch. By measuring these static pressures, the pressure distribution in the swirl flow is estimated. When the pressure gradient is large, the arc becomes stable, so that the conventional torches need large flow rate to increase the centrifugal force for the stable arcing. This results in the arcjet having low specific energy and degrades the cut quality.

The structure of the swirl flow depends mainly on the nozzle shape, so that it is very important to determine its shape to create the maximum pressure gradient under the

*Komatsu Ltd.
**Communicated by Mitsuharu Masuda (Department of Energy Conversion Engineering)

condition of constant flow rate. Using a large-scale torch model made of acrylic-resin, the pressure distribution in the discharge space was measured for various nozzle models with different shapes. The metal cutting test was also performed to compare the performance of the nozzle with the optimum shape with that of the commercial nozzle of Komatsu G940 torch.

2. The nozzle with a mixing chamber

Figure 1 shows the schematic diagram of the nozzle and cathode, where d is the gap distance between the nozzle wall and the cathode surface, v the exit velocity of the arcjet. The center of the nozzle does not coincide accurately with that of the electrode due to the manufacturing and setting errors. Even the minute defference caused by these errors creates the difference in the gap distance and results in the differences of the velocity and pressure across the nozzle exit. Consequently, the arcjet is deflected according to the magnitude of the difference in concentricity, as it leaves the nozzle. The jet with large deflection causes a cut surface to be inclined and results in unacceptable precision of the cut part[3].

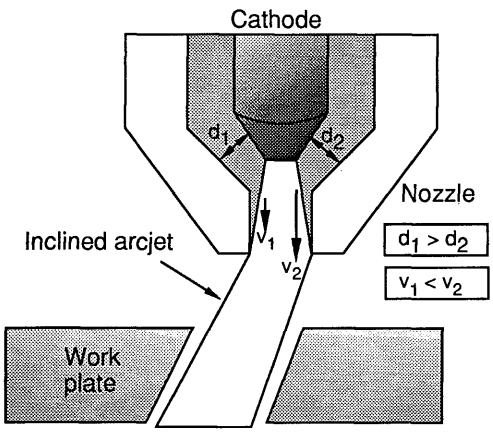

Fig. 1 Schematic representation of the mechanism of jet deviation and the inclined cut surface.

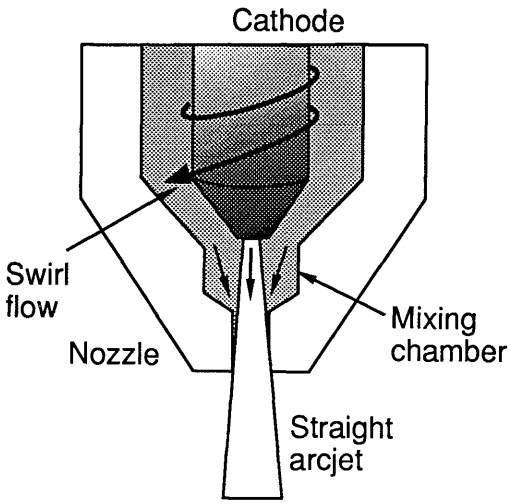

Fig. 2 Mixing chamber.

To solve this serious problem, a mixing chamber[4] was devised to equalize the flow pressure before the plasma leaves the nozzle, as shown in **Fig. 2**. This mixing chamber showed a remarkable effect to prevent the jet deviation[4]. This effect is explained in detail in the latter part of this paper.

Figure 3 shows the cross sectional view of the torch head (Komatsu G940). In this Figure, ΔL is the distance between the top surface of the electrode and the upper surface of the mixing chamber, D the diameter of the mixing chamber, d_1 the entrance length, d_2 the depth of the mixing chamber and d_3 the length of the acceleration being fixed to 3.4 mm in this experiment. The swirler has four equally spaced injection orifices tangential to a

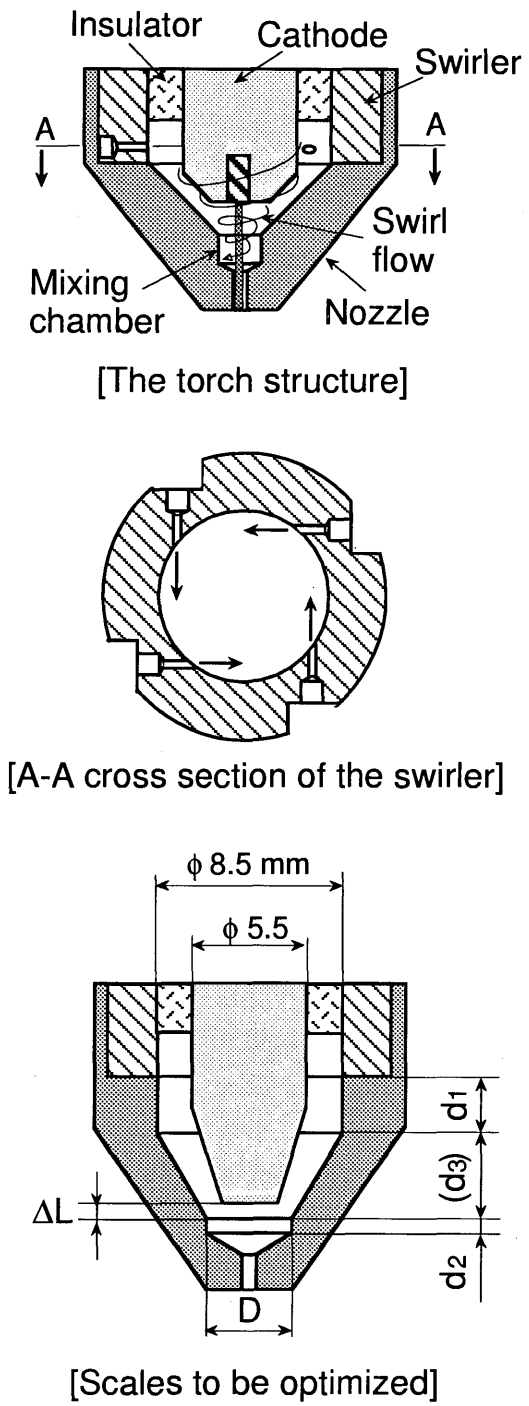

Fig. 3 Torch structure and scale parameters to be optimized.

cylindrical surface and perpendicular to the center axis of the torch.

3. Pressure measurement in the torch with the large-scale model

Figures 4 and **5** show the schematic diagrams of the large-scale torch model and the measurement system, respectively. In **Fig. 4**, p_e is the static pressure at the center of the top surface of the electrode, p_{vr} the static pressure at the bottom of the wall of the mixing chamber and p_n the static pressures measured by pressure holes equally spaced with an angle of 90° at the middle of the orifice passage. The

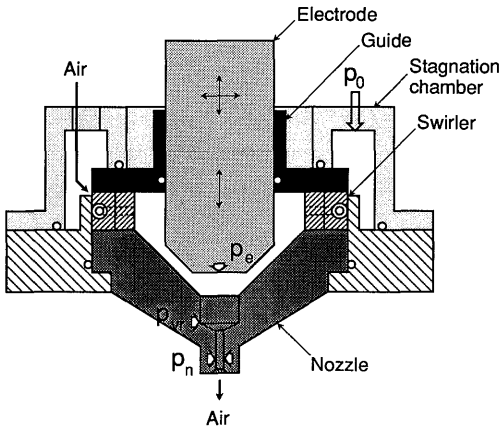

Fig. 4 The large-scale torch model and the measured pressures.

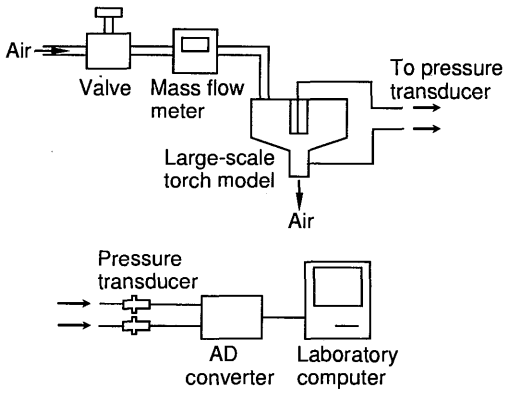

Fig. 5 Pressure measurement system.

maximum difference among the four values of p_n is denoted by dp_n.

The large-scale model is five times larger than the commercial torch (Komatsu G940). Each component of the model can be replaced to test the different geometries for the change in experimental conditions. The electrode position relative to the nozzle is adjustable in horizontal and vertical direction to simulate the manufacturing and setting errors. The distance between the center of the nozzle and electode is denoted by Δr.

The gas flow rate necessary for this model experiment was estimated by considering that the Reynolds number of the flow inside the model was equal to that of the actual torch.

To measure the static pressures at each point in the model, small holes with 0.3 mm in diameter are drilled on the walls of the nozzle and electrode as shown in **Fig. 4**. These are connected to the pressure transducers for automated data acquisition with a laboratory computer as shown in **Fig. 5**.

The location of the pressure holes is determined by the following two considerations. Firstly, the large centrifugal force of the swirl flow makes the p_e small and the p_{vr} large. Secondly, the dp_n is a measure of the nonuniformity of the pressure distribution on the orifice exit plane; when the value of dp_n is zero, the arcjet can be regarded as straight and no flow deviation occurs.

4. Results and discussion

The experimental results obtained with the large-scale torch model by the present pressure measurement system are described in this chapter. All the symbols used in the following figures are consistent with the notations in **Figs. 3** and **4**.

4.1 Effect of the mixing chamber

To clarify the effect of the mixing chamber experimentally, the values of dp_n are measured for two different nozzles. One has a mixing chamber with d_1=11.8 mm, d_2 =3.0 mm, D=20.0 mm and ΔL=0.0 mm and the other a simple conically convergent nozzle with the same length and exit diameter. **Figure 6** shows the dp_n as a function of the distance Δr between the center of the nozzle and electrode, where m is the mass flow rate of the working gas. It is clear from this figure that the mixing chamber has a distinct effect for equalizing the pressure difference.

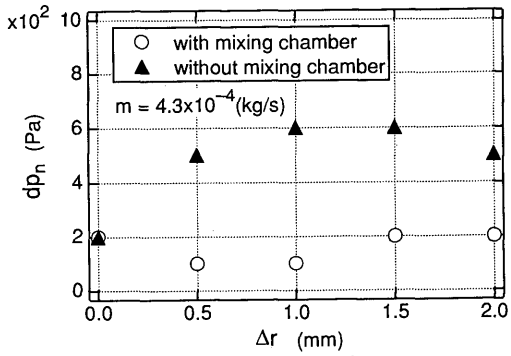

Fig. 6 Effect of the mixing chamber on dp_n as a function of Δr.

4.2 Effect of the displacement ΔL between nozzle and electrode

To clarify the effect of the relative position of the nozzle and the electrode, the effect of ΔL on the pressure distribution was investigated for d_2=1.5 and 3.0 mm. **Figure 7 (a)** to **(c)** shows the plots of p_e, p_{vr} and dp_n as a function of ΔL. This figure indicates; (i) for d_2=3.0 mm, the best condition (dp_n minimum) is obtained at ΔL=0; (ii) for d_2=1.5

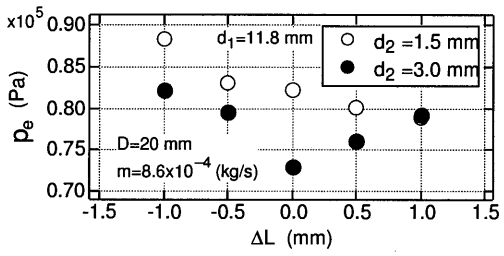

Fig. 7 (a)

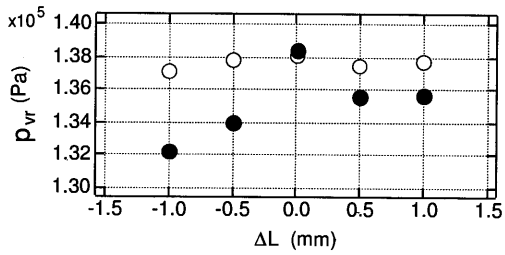

Fig. 7 (b)

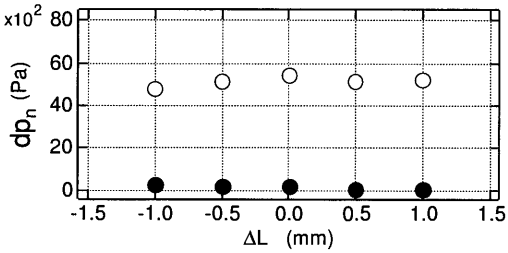

Fig. 7 (c)

Fig. 7 Pressure profiles for different d_2 as a function of ΔL.
(a) p_e vs. ΔL (b) p_{vr} vs. ΔL (c) dp_n vs. ΔL

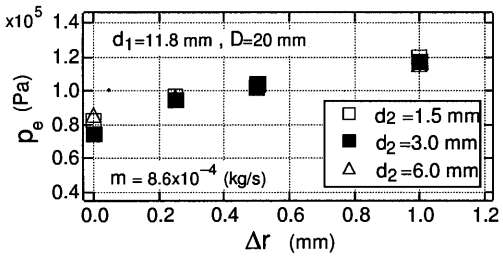

Fig. 8 (a)

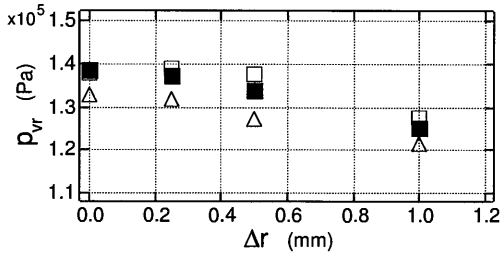

Fig. 8 (b)

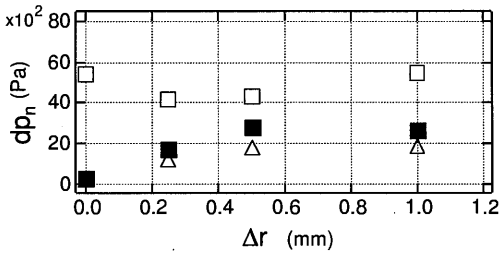

Fig. 8 (c)

Fig. 8 Pressure profiles for different d_2 as a function of Δr.
(a) p_e vs. Δr (b) p_{vr} vs. Δr (c) dp_n vs. Δr

mm, almost no effect is seen to decrease the balue of dp_n. This indicates that the desirable flow condition can be obtained when ΔL is zero and d_2 is greater than or equal to 3.0 mm.

4.3 Effect of the mixing chamber depth d_2

To determine the optimum value of d_2, the pressures were measured by varying d_2. **Figure 8 (a)** to **(c)** shows the measured pressures p_e, p_{vr} and dp_n as a function of Δr. Clearly, the pressure difference dp_n for $d_2=1.5$ mm differs from the other two data. This means that the mixing chamber does not work properly when the d_2 is excessively small. Although there is no remarkable difference between the data for $d_2=3.0$ and 6.0 mm, the p_{vr} is small for the large d_2. This tendency may generate an unstable arc such as caused by kink instability.

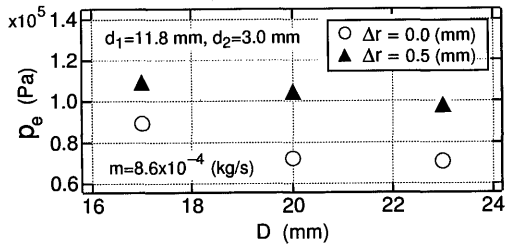

Fig. 9 (a)

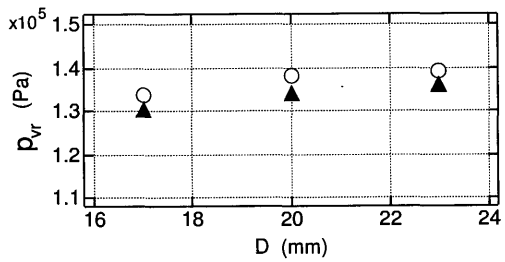

Fig. 9 (b)

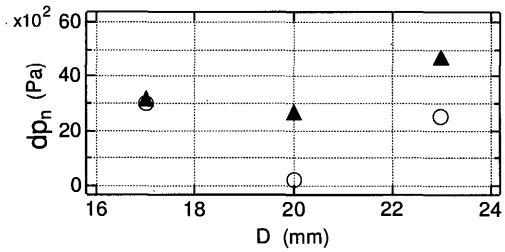

Fig. 9 (c)

Fig. 9 Pressure profiles for different Δr as a function of D.
(a) p_e vs. D (b) p_{vr} vs. D (c) dp_n vs. D

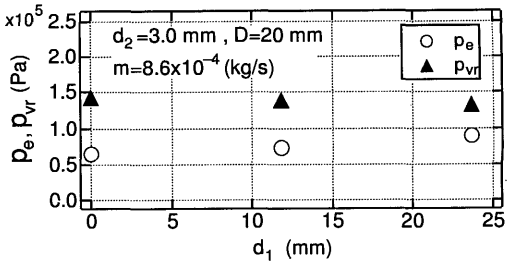

Fig. 10 (a)

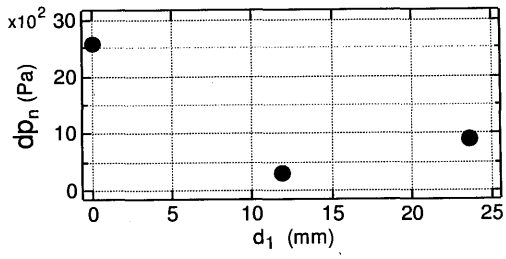

Fig. 10 (b)

Fig. 10 Pressure profiles as a function of d_1 for $d_2 = 3.0$ mm and $D = 20$ mm. (a) p_e, p_{vr} vs. d_1 (b) dp_n vs. d_1

4.4 Effect of the mixing chamber diameter *D*

Figure 9 (a) to **(c)** shows the p_e, p_{vr} and dp_n as a function of the diameter of the mixing chamber for $\Delta r = 0.0$ and 0.5 mm. In this figure, the dp_n has a minimum value at $D = 20$ mm. These results strongly suggest that there exists an optimum value of D.

4.5 Effect of the entrance length d_1

Figure 10 (a) and **(b)** shows the effect of d_1 on the measured pressures. The p_e and p_{vr} are found to change linearly with d_1. The large d_1 decreases the centrifugal force of the swirl flow by its large frictional loss. This figure also shows that there exists a minimum value of dp_n at $d_1 = 12$ mm.

5. The cutting performance with the optimized nozzle

To examine the validity of the experimental results obtained with the large-scale torch model and the pressure measurement system, the nozzle was made that had a similar size with the plasma cutter and was optimized according to the results of the present experiments. This nozzle was tested in the actual cutting process. The double arcing was caused directly by the arc instability inside the torch and could be used as a measure of the cutter performance. Therefore, the total number of the double arcing occurred during the cutting process was selected as a parameter for the evaluation. The test was performed by cutting the carbon-steel plate with the thickness of 1.6 mm under the condition of dross-free cutting[2]. **Figure 11** and **Table 1** show the test results and the nozzle specifications used in this test, respectively. In the figure, ϕ is the exit diameter of the nozzle, I the arc current and p_0 the supply pressure of the working gas. In the table, the optimized nozzle is denoted by "Proto" and the conventional nozzle by "G940". The same test procedure was repeated three times for these two nozzles. These results confirm the performance of the optimized nozzle superior to that of the conventional one.

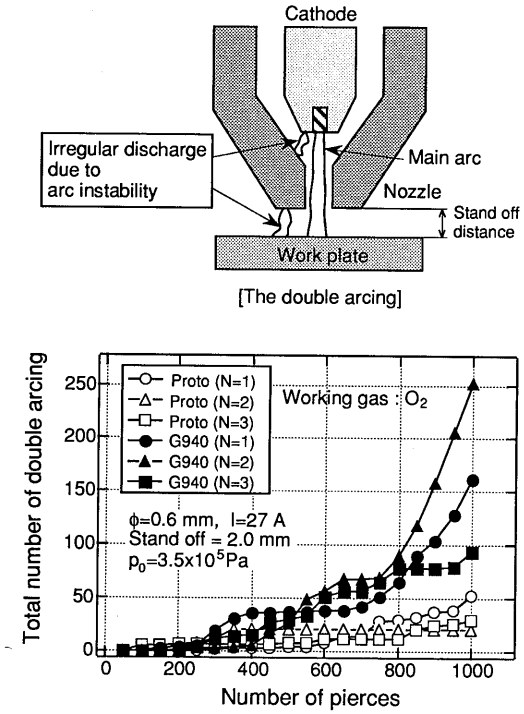

Fig. 11 Schematic representation of the double arcing, and the total number of the double arcing during 1000 times of cutting operation for the two types of nozzles.

Table 1 Nozzle specifications used in the cutting test.

	ΔL (mm)	D (mm)	d_1 (mm)	d_2 (mm)	d_3 (mm)
Proto	0.0	4.0	2.4	0.6	3.4
G940	1.0	2.0	0.0	1.5	3.4

6. Conclusions

The optimum nozzle geometry for a plasma cutting torch was studied by using a large-scale torch model. The pressure measurement inside this model gives the method to determine an optimized geometry. The nozzle shape obtained by the present work shows a superior performance in arc stabilization inside the torch to the conventional torch. Also, the present plasma torch can be operated with sufficiently high specific energy, ans has remarkable effects on the stable dross-free cutting.

Acknowledgement

The author is grateful to Mr. N, Tsurumaki for his assistance in the experimental work.

References

1) NASA SP-5033 Technology Survey "Plasma Jet Technology" Oct. 1965
2) Sakuragi, S., "The characteristics and structure of a transferred arcjet for dross-free plasma cutting", Engineering Sciences Reports, Kyushu University, Vol. 16, No. 4, pp. 387-392, March 1995.
3) White, J., "Cutting with precision plasma technology" The Fabricator, May 1993.
4) Sakuragi, S., "Transferred plasma arc torch", U. S. Patent. No. 5, 214, 263, May 25, 1993.